Five Level Cascaded H-Bridge D-STATCOM using a new Fuzzy and PI Controllers model for Wind Energy Systems

Kenan YANMAZ[1], Ismail Hakki ALTAS[2], Onur Ozdal MENGI[3]
[1]*Vocational School of Technical Sciences, Giresun University, Giresun, 28200, Turkey*
[2]*Electrical and Electronics Engineering, Karadeniz Technical University, Trabzon, 61080, Turkey*
[3]*Energy Systems Engineering, Giresun University, Giresun, 28200, Turkey*
kenan.yanmaz@giresun.edu.tr

Abstract—**Power quality is one of the important issues in wind energy systems as in all renewable energy systems. Reactive component of current in distribution systems causes negative effects on the network, including power loses, voltage drop, and reduced line capacity. Static Synchronous Compensator (STATCOM) has been used increasingly instead of conventional devices such as switched capacitor groups and Static Var Compensator (SVC) to improve the power quality. Flexible AC Transmission System (FACTS) devices such as STATCOM are also used in power distribution systems and called Distribution STATCOM (D-STATCOM). D-STATCOM is used to improve the power quality in distribution systems as an inverter based device. Fixed parameter conventional PI controllers are usually used to control D-STATCOM devices. D-STATCOM device used in a wind power distribution system has a voltage-controlled inverter structure based on a five-level H-bridge topology. A new indirect current control scheme based on synchronous reference frame theory is proposed to produce gate pulses that are needed for the inverter. A fuzzy adaptive PI controller (FLCM-PI) is designed and used in the control scheme such that the parameters of the PI controller are modified by a fuzzy logic controller (FLC) to adapt the operation for changing conditions. The D-STATCOM topology with the proposed controller is simulated and experimentally tested.**

Index Terms—**wind energy, flexible AC transmission systems, current control, fuzzy logic, proportional control.**

I. INTRODUCTION

Wind Energy Conversion Systems (WECS) have an important role as a renewable energy source. They produce energy by using wind power [1]. The WECS must be controlled continuously due to changes in wind speed. In order to connect the WECS to electrical loads, interfacing devices such as rectifiers and inverters must be used. However, these power electronic devices generate harmonics, which must be eliminated. The asynchronous generators used in wind turbines operating in standalone mode require excitation capacitors [15]. Besides, harmonics are not only caused by the power electronic converters, it is also caused by switched mode loads on the load side. Therefore the WECS are different from conventional power stations and require additional precautions to be taken for eliminating harmonics and maintaining the energy sustainability. To eliminate these problems, FACTS devices

are used [2]. These FACTS devices are used with advanced compensation techniques.

Techniques containing systems such as D-STATCOM, STATCOM and SVC with advanced power electronics, is adapted to distribution systems [3]. Correction of voltage amplitude and the elimination of harmonics are both provided by this method. The reactive power is also controlled by this technique. Electrical machines cause by inductive effects because of their windings and these effects are resolved through the capacitors, which are a part of D-STATCOM structure and used for compensation as well as for the harmonic elimination [4].

In the literature, many wind turbine emulators are used. Most of the emulator are created by using squirrel cage induction machines, synchronous machines, permanent magnet direct current machines [5-8].

Various methods are used to control D-STATCOM consisting of voltage-controlled inverter [9]. Another one with a multi-level structure using different types power electronics schemes [10, 11]. Indirect current control method based on synchronous reference frame theory has been used for the D-STATCOM control [12-14]. Within these structures, PI and fuzzy-PI based controllers for two-level inverter are used [12-16].

The choice of modulation technique is also important in STATCOM control system. In the literature, different Pulse Width Modulation techniques such as Carrier-based Pulse Width Modulation [17], multi-level space vector modulation [18] and selected harmonic elimination pulse width modulation [19, 20] are used.

In this study, the reactive power compensation is done by examining structure of the D-STATCOM in the network-independent island-type wind turbine system by using a model based on wind turbine emulator. D-STATCOM contains 5-level voltage source inverter. The scheme is examined by using PI and FLCM-PI controller and the results are compared. System simulation is done in MATLAB / Simulink environment.

Five level cascaded H-bridge based voltage source inverter is used here. More precise control is possible with the increase of level of the inverter. However, it becomes more difficult to control the system accordingly due to increased number of switching elements. This delicate structure in the system is formed by using the 24 IGBT. Increasing the number of elements in the upper levels

increases system cost, which is not preferred [21-23].

The objective of this paper is to introduce a new approach to control the three phase cascaded H-bridge five level inverter based D-STATCOM for wind energy systems. This nonlinear and robust control algorithm based FLCM-PI enhances the transient response of the D-STATCOM for providing power factor correction and achieve a good dynamic response under different load conditions. At the same time a transformerless D-STATCOM system based on five level cascaded H-bridge voltage source inverter is presented and experimentally performed, therefore, enabling the elimination of costly, heavily, and bulky transformer [24]. This line frequency transformer conduces to power losses. Good dynamic system response is achieved with Phase Opposition Disposition-Sinusoidal PWM (POD-SPWM) based inverter operating low switching frequency.

This paper is organized as follows. As the first step the system is simulated in Matlab/Simulink environment. Then, the simulation results are compared with experimental system results. The performance of three-phase D-STATCOM is validated for power quality enhancement with different loads by hardware implementation using dSPACE DS1104 controller board. The effectiveness of the proposed approach are verified through both simulation and experimental studies.

II. CASCADED H-BRIDGE FIVE LEVEL INVERTER BASED D-STATCOM

Fig. 1 shows an overview of the proposed system. As shown in Fig. 1, structure of D-STATCOM used to control power to the load from the wind turbine, consists of five-level cascaded H-bridge-based voltage source inverter, DC-link capacitors that meet the DC voltage that is required for the inverter circuit, control circuit for the switching, and inductance of a connection.
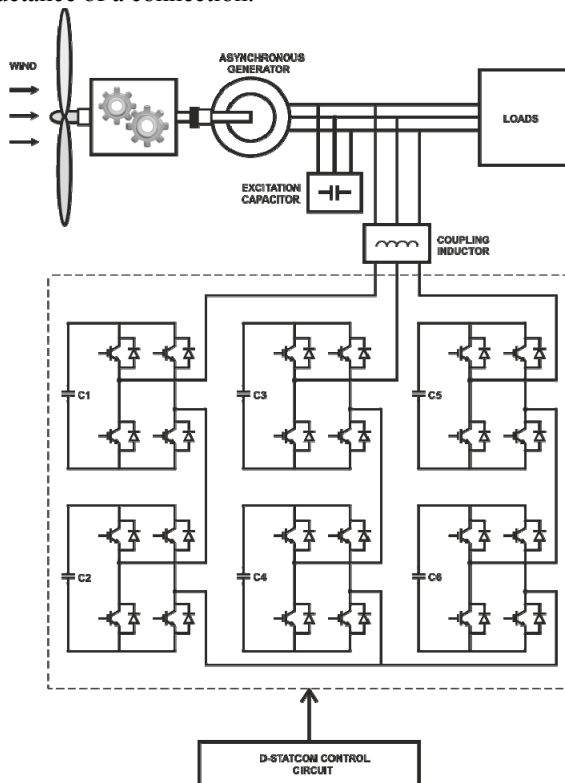

Figure 1. System structure with D-STATCOM

A schematic diagram of the five-level inverter is shown in Fig. 1, where there are 6 H-bridge in total including 2 in each phase. Each phase voltage of the inverter is the sum of the output voltage in the respective phase of each H-bridge. The D-STATCOM is connected in parallel to the power system. A serial port connection inductance (Z_{st}) is used to ensure this connection in the common port. The size of the reactive current (i_{st}) flowing toward the connection inductance is proportional to the difference of D-STATCOM AC output voltage (v_{st}) and voltage at a common connection point (v_{pcc}). This is achieved by controlling the amplitude of the voltage of the DC link capacitors (v_{dc}).

The solution of the equations in ABC coordinate axis control system is difficult and complicated in terms of design steps, because the variables on the AC side of the mathematical model are time-dependent. Therefore the equations are converted to two-phase d-q coordinate axis using Park's transformation. The transformation matrix given in (1) is used to transform the equations from three phase ABC system to two-phase d-q axis rotating simultaneously.

$$T = \sqrt{\frac{2}{3}} \begin{bmatrix} cos\theta & cos(\theta-2\pi/3) & cos(\theta+2\pi/3) \\ -sin\theta & -sin(\theta-2\pi/3) & -sin(\theta+2\pi/3) \\ \frac{1}{\sqrt{2}} & \frac{1}{\sqrt{2}} & \frac{1}{\sqrt{2}} \end{bmatrix} \quad (1)$$

The transformation matrix T is used as $i_{stdq}=T*i_{abc}$ to transform three phase currents from ABC axes frame to d-q axes frame.

Then, the D-STATCOM current is written in terms of the currents in d-q axes as in (2).

$$i_{st} = \pm i_{std} \pm j i_{stq} = i_{st} < \pm\varphi \quad (2)$$

Where φ; phase difference between i_{st} and v_{pcc}, i_{std}; active current used for charging / discharging status and i_{stq}; link inductance and reactive current flowing to Z_{st}.

A PLL is used to calculate the phase angle of the source voltage required for the load current i_{lq}, D-STATCOM output current and voltage to be converted to d-q axes. Then the controller generates switching signals to drive the switching elements of the inverter. POD-SPWM technique was used to produce these switching signals.

The state equations of D-STATCOM in d-q axis is given in (3).

$$\begin{bmatrix} v_{std} \\ v_{stq} \end{bmatrix} = \begin{bmatrix} v_{pccd} \\ v_{pccq} \end{bmatrix} - L_{st}\frac{d}{dt}\begin{bmatrix} i_{std} \\ i_{stq} \end{bmatrix} - \omega L_{st}\begin{bmatrix} i_{stq} \\ -i_{std} \end{bmatrix} \quad (3)$$

Equation (3) is combined for current samples n and $n+1$ and divided to T_{istd} and T_{istq}. The average magnitude of the voltage vector is derived as in (4) and (5).

$$v_{std}(n,n+1) = $$
$$v_{pccd}(n,n+1) - \frac{L_{st}}{T_{istd}}(i_{std}(n+1)-i_{std}(n)) - \omega L_{st} i_{stq}(n,n+1) \quad (4)$$

$$v_{stq}(n,n+1) = $$
$$v_{pccq}(n,n+1) - \frac{L_{st}}{T_{istq}}(i_{stq}(n+1)-i_{stq}(n)) + \omega L_{st} i_{std}(n,n+1) \quad (5)$$

A fast and accurate response of the controller is always required in D-STATCOM applications. Therefore, the output current of D-STATCOM in the next sample is

requested to monitor current reference in the instant sample.

$$i_{std}(n+1) = i_{std\_ref}(n) \qquad (6)$$

$$i_{stq}(n+1) = i_{lq}(n) \qquad (7)$$

The change in the variables from one sampling instant to the next one, for example from sample *n* to *n+1*, shows a linear behavior.

$$i_{std}(n,n+1) = (i_{std\_ref}(n) + i_{std}(n))/2 \qquad (8)$$

$$i_{stq}(n,n+1) = (i_{lq}(n) + i_{stq}(n))/2 \qquad (9)$$

Network voltage and D-STATCOM output voltage is considered as equal to reference voltage and constant during a sampling period.

$$v_{pccd}(n,n+1) = v_{pccd}(n) \qquad (10)$$

$$v_{pccq}(n,n+1) = v_{pccq}(n) = 0 \qquad (11)$$

$$v_{std}(n,n+1) = v_{std\_ref}(n) \qquad (12)$$

$$v_{stq}(n,n+1) = v_{stq\_ref}(n) \qquad (13)$$

Equations (6) – (13) are substituted into (4) and (5) to obtain *d-q* reference voltage values as (14) and (15).

$$v_{std\_ref}(n) =$$
$$v_{pccd}(n) - K_{id}(i_{std\_ref}(n) - i_{std}(n)) - \omega L_{st}(i_{lq}(n) + i_{stq}(n))/2 \qquad (14)$$

$$v_{stq\_ref}(n) =$$
$$-K_{iq}(i_{lq}(n) - i_{stq}(n)) + \omega L_{st}(i_{std\_ref}(n) + i_{std}(n))/2 \qquad (15)$$

Where controller gain values:

$$K_{i(d,q)} = \frac{L_{st}}{T_{ist(d,q)}} \qquad (16)$$

Thus desired D-STATCOM output voltage and its phase angle, are defined as in (17) and (18), respectively.

$$v_{st\_ref} = \sqrt{(v_{std\_ref})^2 + (v_{stq\_ref})^2} \qquad (17)$$

$$\delta = \tan^{-1}\left(\frac{v_{stq\_ref}}{v_{std\_ref}}\right) \qquad (18)$$

As in Fig. 1, capacitors in each branch of the H-bridge are used as the energy storage elements. The sum of these capacitor voltages are organized according to system requirements and used in active reference current in the voltage control loop.

$$I_{DC} = C\frac{dV_{DC}}{dt} \qquad (19)$$

Where *C* is the sum of the capacitors of two branches in H-bridge inverter where the flowing current I_{DC} flows through. Equation (20) is obtained if the (19) is re-written in *d-q* coordinate axes.

$$I_{DC\_dq} = C\frac{dV_{DC\_dq}}{dt} \qquad (20)$$

q-axis component can be ignored since only *d*-axis current component is needed for charging and discharging the DC-link capacitor. The average amplitude of the active current vector is obtained as in (21) by getting the average value of (20) over a sampling period (T_{vdcd}).

$$I_{DC\_d}(n,n+1) = \frac{C}{T_{vdcd}}V_{DC\_d}(n,n+1) \qquad (21)$$

In the next sample the DC-link capacitors against the total DC reference voltage is found by equalization.

$$V_{DC\_d}(n+1) = V_{DC\_d\_ref}(n) \qquad (22)$$

The DC current is considered constant and equal to the reference current in a sampling period.

$$I_{DC\_d}(n,n+1) = i_{std\_ref}(n) \qquad (23)$$

Substituting (22) and (23), in (21) final reference current value is obtained as the one in (24).

$$i_{std\_ref}(n) = \frac{C}{T_{vdcd}}\left[V_{DC\_d\_ref}(n) - V_{DC\_d}(n)\right] \qquad (24)$$

The control voltage coefficient becomes as in (25) if DC reference voltage is 1 p.u.

$$K_{p\_vd} = \frac{C}{T_{vdcd}} \qquad (25)$$

III. FUZZY LOGIC CONTROLLER

As shown in Fig. 2, fuzzy logic controller consists of the fuzzifier, rule base, fuzzy inference and defuzzifier. Fig. 3 shows the simulink model of FLC [25]. Fuzzifier, the first subsystem of the FLC, converts the exact input values of error (*e*) and change in error (*de*) to fuzzy values. For this block triangle membership functions are used. These fuzzy values are sent to fuzzy rule base unit and processed with fuzzy rules by using Mamdani's max-min method in fuzzy inference [26].
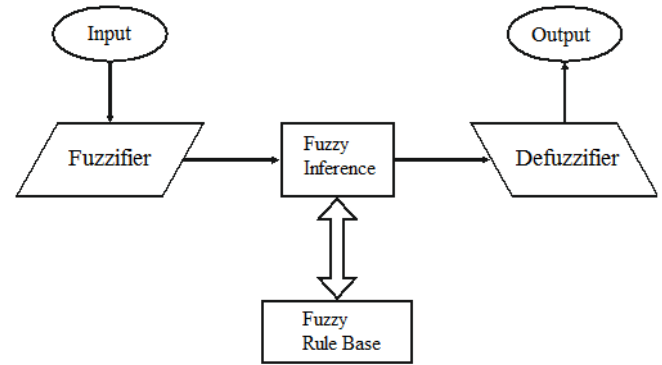

Figure 2. Fuzzy logic controller scheme

These final fuzzy values are sent to defuzzifier unit of FLC. Finally, in this subsystem the fuzzy results are converted to exact output values using the center of area method [27].

The models of all FLC's units are improved in Matlab/Simulink environment (without using FLC Toolbox) [30]. As shown in Table I, FLC used in this system has 25 rules. The operation with 9 or 49 rules are also tested. However, FLC with 9 rules could not satisfy the desired system performance while FLC with 49 rules give the same performance as 25 rules. Detailed information is given in reference [25].

TABLE I. RULE TABLE

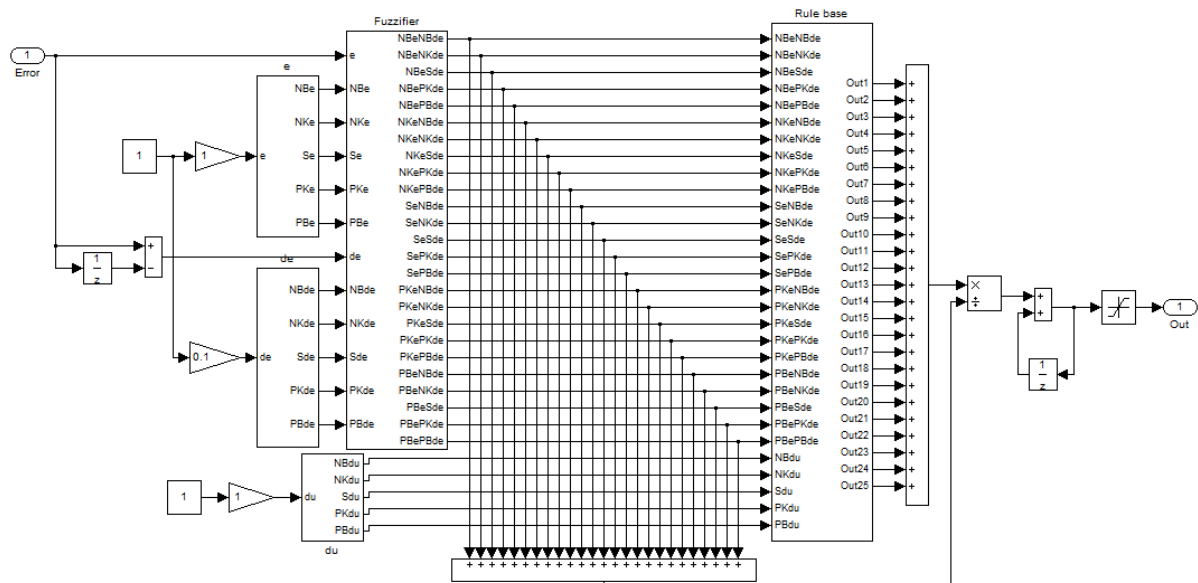| de \\ e	NB (Negative Big)	NS (Negative Small)	Z (Zero)	PS (Positive Small)	PB (Positive Big)
NB	NB	NB	NS	NS	Z
NS	NB	NS	NS	Z	PS
Z	NS	NS	Z	PS	PS
PS	NS	Z	PS	PS	PB
PB	Z	PS	PS	PB	PB

Figure 3. Simulink model of FLC

IV. FLCM-PI CONTROLLER

FLCM-PI controller means that the two parameters *Kp* and *Ki* of PI controller are tuned by using FLCM. The coefficients of the conventional PI controller are set and kept constant [28]. They are not adaptive and do not updated for changing conditions. In some applications, the controller parameters are often tuned for the nonlinear plant with undesired parameter variations. Therefore, it is necessary to automatically tune the PI parameters. FLCM-PI controller is a PI controller that employs the FLC to tune the parameters *Kp* and *Ki* according to error and change of error [29]. Since the parameters of the PI controller are modified by an FLCM. The structure of the FLCM-PI controller is shown in Fig. 4.
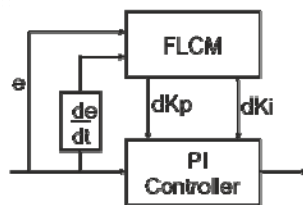
Figure 4. Block diagram of the FLCM-PI controller

V. PROPOSED CONTROL STRATEGY FOR CASCADED H-BRIDGE FIVE LEVEL INVERTER BASED D-STATCOM

Block diagram of a synchronous reference frame theory indirect current control system for D-STATCOM obtained from (17), (18) and (24) is shown in Fig. 5. The proposed controller consists of three main elements. The first of these elements is to keep the DC voltages of each H-bridge capacitors balanced. The second element is to control the D-STATCOM current for the reactive and active power transferred to the main systems. The third elements of the proposed controller is to generate required PWM signals.

The sum of each separated DC capacitor voltage levels is kept constant in the control system and reference voltage needed to be produced by the inverter is obtained based on reference active and reactive power. For this DC capacitor voltage control, PI controllers are often used but have some inconveniences in terms of settling time and overshoot.
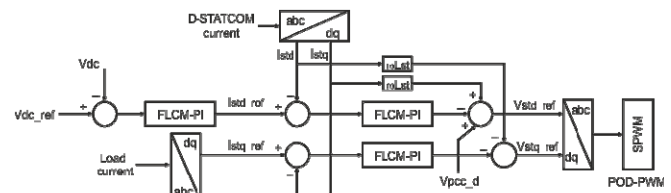

Figure 5. Block diagram of D-STATCOM controller

For example in [31], PI controllers were used to control voltage and current for nine level cascaded voltage source converter based STATCOM system. In steady state operation, instability of the control system, poor transient response, high settling time, maximum overshoot and the oscillation of the reactive current can be seen. In [32], PI controller may not be sufficient due to the variety of parameters. In [33], PI controller was used for DSTATCOM. With decoupled current control based PI controller, harmonic compensation capability is above the IEEE Std. harmonic current limit and DC voltage is poor in terms of maximum overshoot.

Since FLCM-PI controller shows a correction and fast response, it has been selected in this paper to reach rapid and robust control of the DC-link capacitor voltage.

The actual load connected to the experimental system is measured by means of the designed sensors and transferred to the control system by dSPACE DS1104 controller board. This load reactive current is sent to the control system to correct the power factor of the power system. It is desirable that the difference between the D-STATCOM output reactive current and the load reactive current be zero. The oscillation or variation occurs in the D-STATCOM output reactive current for reasons such as the switching elements of the inverter [34], switching frequency of the inverter [35], the tolerance of the DC-link capacitors, and ripple content of the DC-link voltage. FLCM-PI controller is designed to eliminate these problems, get faster response times and get zero steady state error.

The modulation signals obtained from controller system are sent to POD-SPWM block. For five level inverter four triangular carrier signals with same amplitude and frequency

are composed [36]. The modulating signals are compared with these four triangular carrier signals to produce the switching signals. In POD-SPWM technique, the all positive carrier signals are in phase, and the carrier signals below the zero reference are shifted by 180°. The POD-SPWM method enhances the output voltage and reduces the harmonic content of the voltage source inverter and voltage stress on inverter's switching elements [37].

VI. RESULTS AND DISCUSSION

A. Simulation Study

D-STATCOM simulation were conducted with different sample experiments. Matlab / Simulink software package is used to accomplish the simulation. The sampling frequency for the control system has been chosen as 6.5 kHz. 800 Hz frequency is selected for switching elements within the D-STATCOM. These values are chosen to be suitable for real-time operation in progress. All these parameters are shown in Table II.

TABLE II. SYSTEM PARAMETERS

Symbol	Quantity	Value
V	system voltage	Three phase 380 V, 50 Hz
V_{dc}	DC-link voltage	200 V
C_{dc}	DC-link capacitance	4700 μF
f	sampling frequency	6.5 kHz
f_{sw}	switching frequency	800 Hz
R_f	coupling resistance	56 mΩ
L_f	coupling inductance	6 mH
	Load 1	1 kW Resistive
	Load 2	4 kW inductance motor
	Load 3	3 kW Resistive (0.3-1s)
	Load 4	1 kW+5 kVar (0.4-1s)

FLCM-PI was used for V_{dc} control and D-STATCOM output currents control in the D-STATCOM controller.

Fig. 6 shows the response of D-STATCOM during load changes. The reactive component of the load current (i_{lq}) and the reactive component of the D-STATCOM current (i_{stq}) changes are shown in Fig. 6. As shown in Fig. 6, when FLCM-PI is used for Controller, it follows reference better than PI.
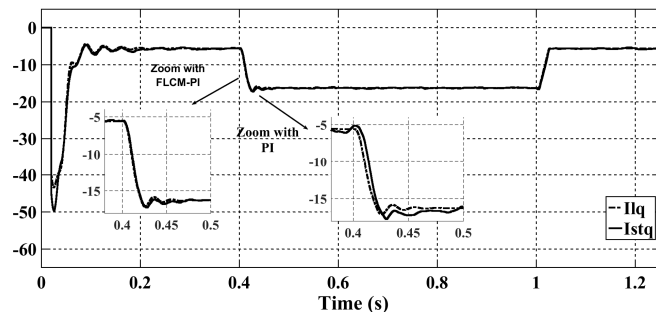

Figure 6. Reactive components of load and D-STATCOM currents

Fig. 7 shows the PCC current d and q components. It is seen that the reactive power is 0 VAr as expected.
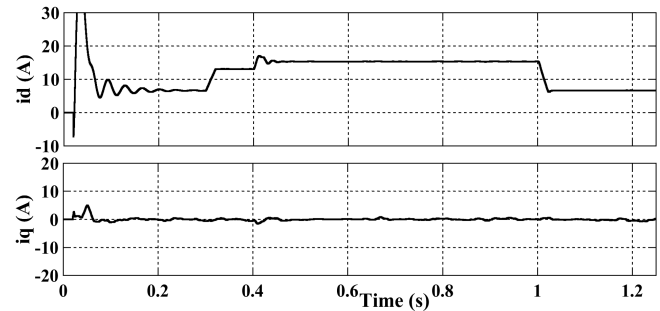

Figure 7. d and q components of the PCC current

Fig. 8 shows the PCC voltage and current variations. It is seen that there is no phase difference between current and voltage for analyzing the power factor.
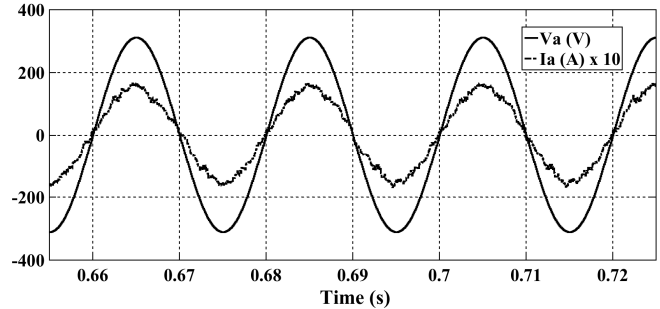

Figure 8. The PCC current and voltage waveforms

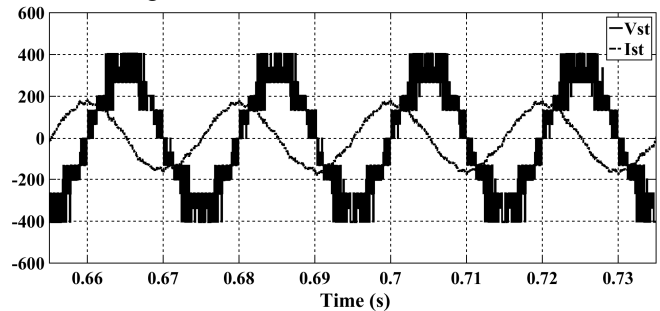Changes of D-STATCOM output current and voltage can be seen in Fig. 9.

Figure 9. Changes of D-STATCOM output current (x10) and voltage

Total voltage variation of each of the H-bridge voltage for a phase of cascaded H-bridge five level inverter-based D-STATCOM is observed in Fig. 10.
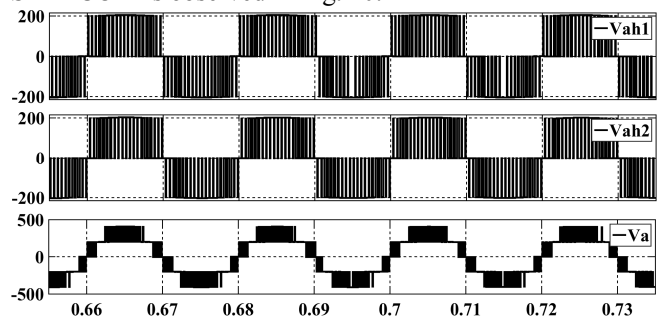

Figure 10. Voltage variation of a phase of D-STATCOM

Total DC-link voltage change of each H-bridge inverter of D-STATCOM is observed in Fig. 11. It is necessary to keep the DC-link voltage constant at 200V.
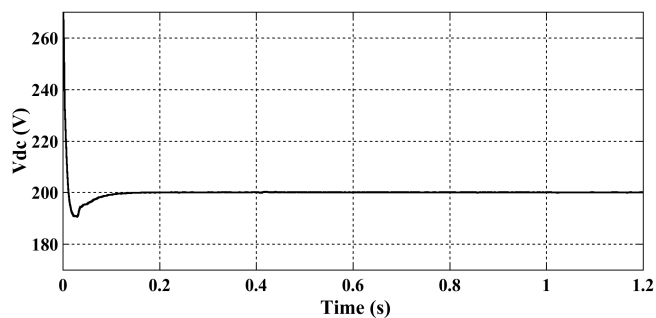
Figure 11. D-STATCOM DC-link voltage change

B. Experimental Setup

A hardware has been built to validate the theoretical implementation and simulation study. Fig. 12 shows a laboratory prototype setup based on a three phase D-STATCOM. There are a total 6 H-bridges with 2 in each phase in five-level inverter structure of D-STATCOM. These H-bridges are constructed using intelligent power modules including insulated gate bipolar transistors. In this experimental setup, there are 6 current sensors (using LA 55-P), 9 voltage sensors (using LV 25-P), dead time circuits, power supplies and measurement devices. A coupling

inductor is connected in series with the inverter preceding to the PCC. A dSPACE DS1104 controller board is used as the main control platform for connection between the hardware and the Matlab/Simulink environment.

Fig. 13 shows the complete control system Simulink diagram for D-STATCOM. This controller scheme is the proposed indirect current control system based on synchronous reference frame theory to produce gate pulses that are needed for the inverter. dSPACE DS1104 enables the connection between the hardware and Simulink model by input output interface blocks. FLCM-PI controller is used for V_{dc} control and PI controller is used for D-STATCOM output current control. This controller performs full reactive power compensation. Switching frequency is fixed. *d-q* axis current of D-STATCOM are independently monitored. The modulation signals used in generating the POD-SPWM signals are obtained from this controller scheme. Fig. 14 shows the POD-SPWM block diagram for switching elements of the inverter. Experimental results are analyzed for transient response, steady state, and power factor correction.
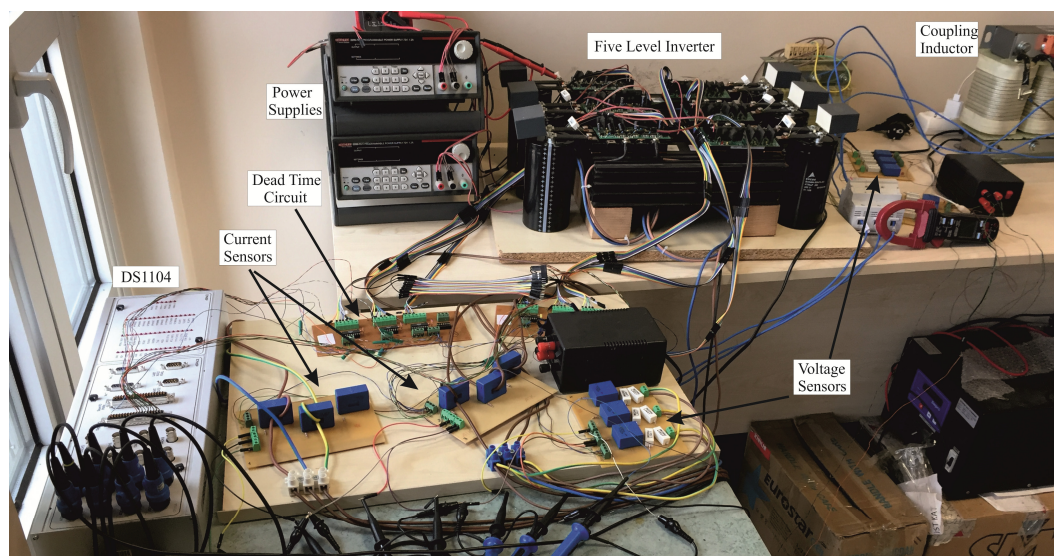

Figure 12. Experimental setup of D-STATCOM consisting of five-level cascaded H-bridge-based voltage source inverter.
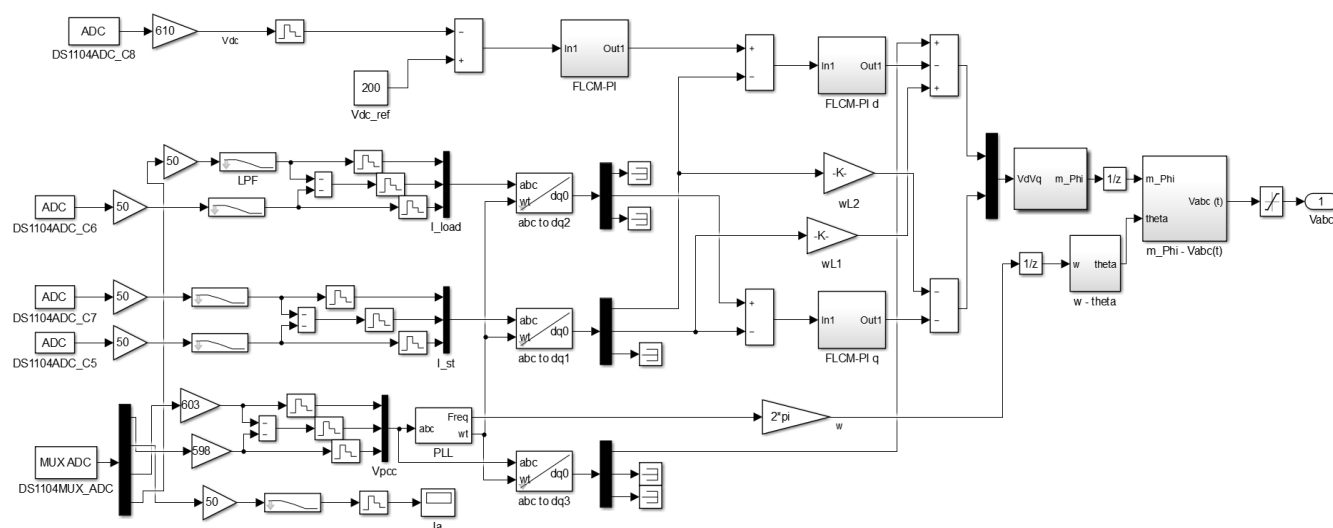

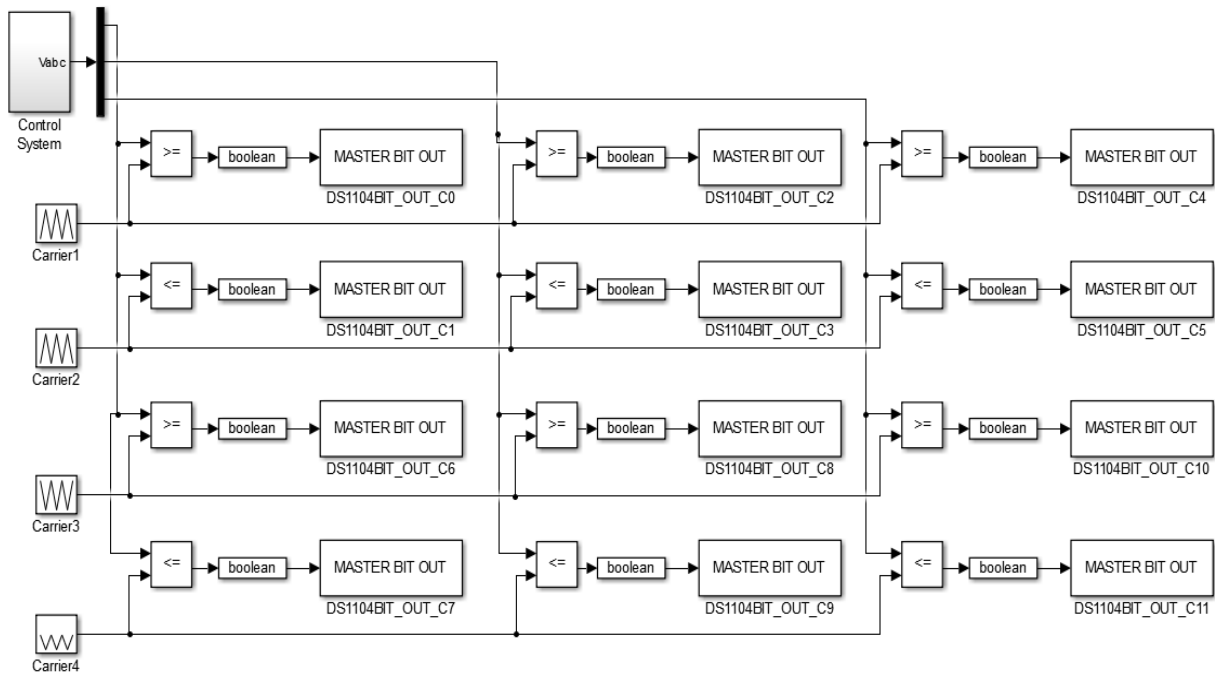Figure 13. The complete D-STATCOM control system Simulink diagram for experimental study.

Figure 14. The block diagram of the POD-SPWM for switching elements of the inverter used in the experimental study.

1) Experimental Study 1

For this experimental study, the sampling time for the control system has been chosen as 263μs and 625 Hz frequency is selected for switching elements within the D-STATCOM. FLCM-PI controllers are used to control D-STATCOM system. For the reference, DC-link voltage is selected as 200 V. The behavior of the complete system can be monitored in real time with the application of the dSPACE ControlDesk graphical user interface software. The variables used in the experimental study were used in the simulation study.

Fig. 15 shows the voltage response of PCC for both simulation and experimental study.
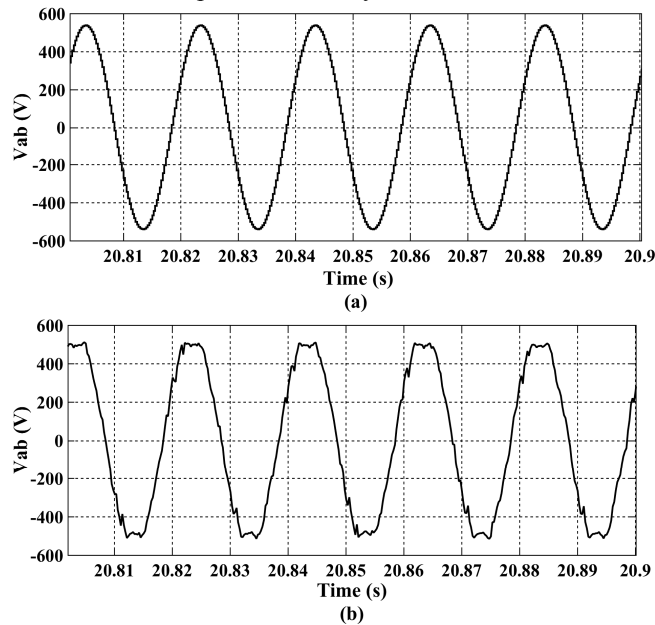

Figure 15. PCC voltage waveform (a) simulation study (b) experimental study

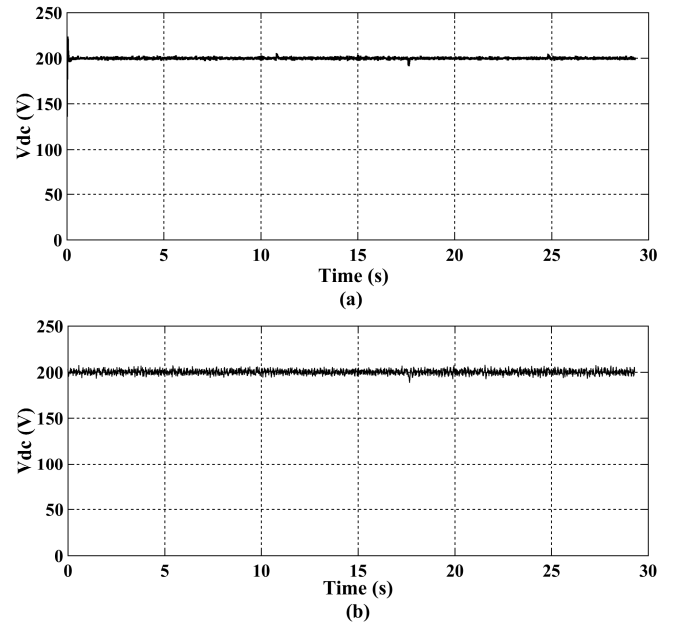Fig. 16 shows the separate DC-link capacitor voltage waveform of each H-bridge inverter.

Figure 16. (a) Simulation (b) experimental waveform of DC-link voltage

Fig. 17 shows the dynamic response of D-STATCOM current. As shown in Fig. 17, reference reactive current of load (i_{lq}) is changed from 0 to 10A (capacitive reactive load), 10A to -10A (inductive reactive load) and -10A to 0 by using the dSPACE control desk. q axis current of D-STATCOM (i_{stq}) is tracking i_{lq}.
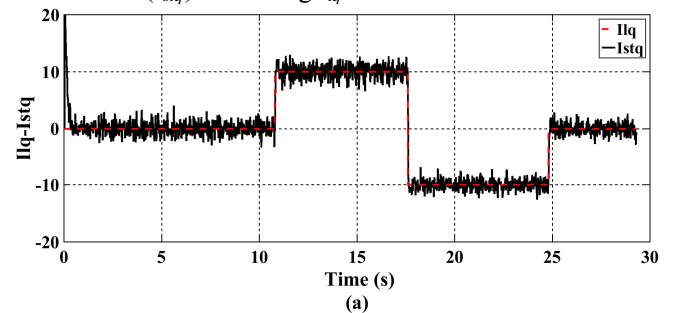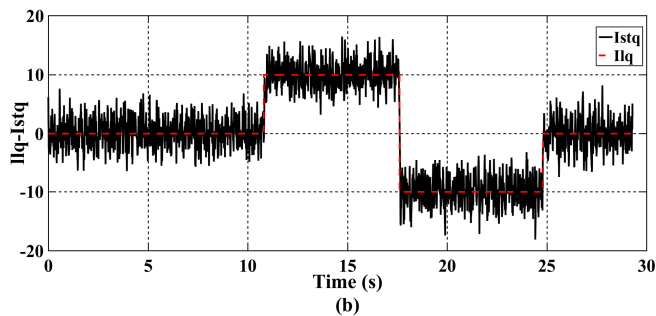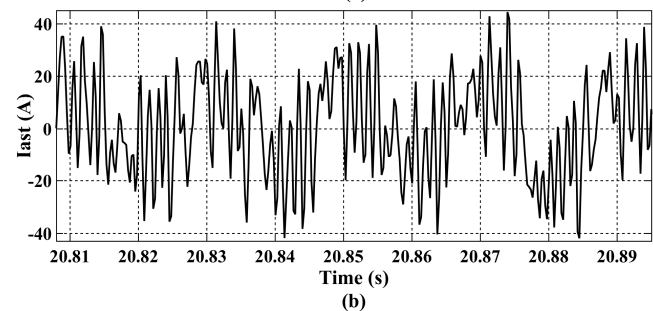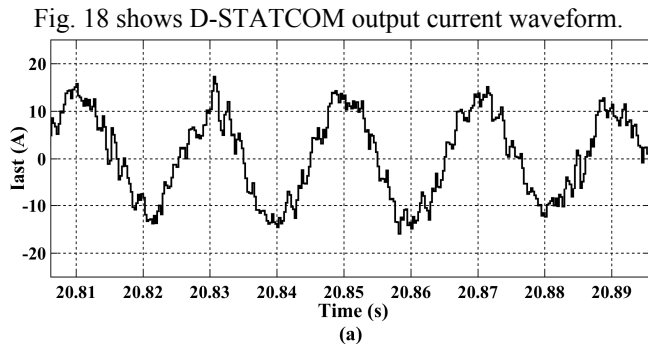
Figure 17. (a) Simulation (b) experimental waveform of i_{lq} and i_{stq}

Fig. 18 shows D-STATCOM output current waveform.

Figure 18. (a) Simulation (b) experimental waveform of D-STATCOM output current

2) Experimental Study 2

For another experimental study, the sampling time for the control system has been chosen as Ts=300μs and fsw=833 Hz frequency is selected for switching elements within the D-STATCOM. POD-SPWM with a frequency of 833 Hz is considered as a modulation technique for voltage source inverter. FLCM-PI controllers are used to control D-STATCOM system. For the reference, DC-link voltage is selected as 200 V. A coupling inductor of 20mH instead of 3mH is connected between the D-STATCOM and the PCC. The behavior of the complete system can be monitored in real time with the application of the dSPACE ControlDesk graphical user interface software.

Fig. 19 shows the individual DC-link capacitor voltage waveform of each H-bridge inverter. Fig. 20 shows D-STATCOM output current waveform. Fig. 21 shows the voltage response of PCC.
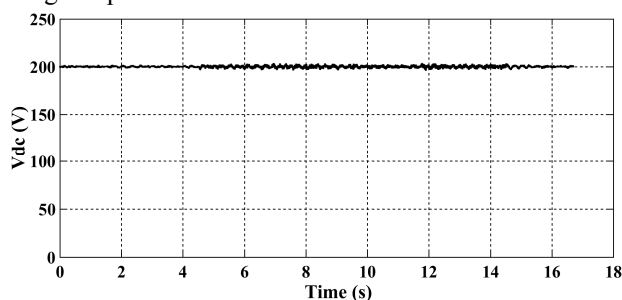
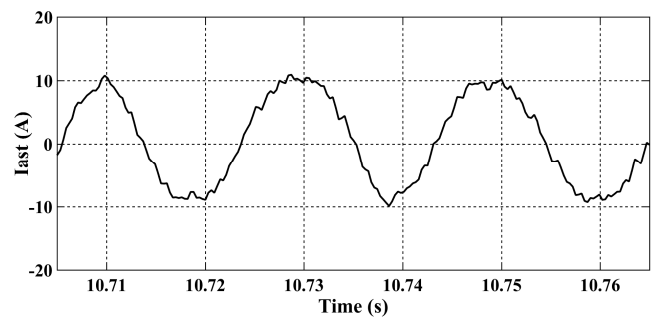Figure 19. Experimental waveform of DC-link voltage

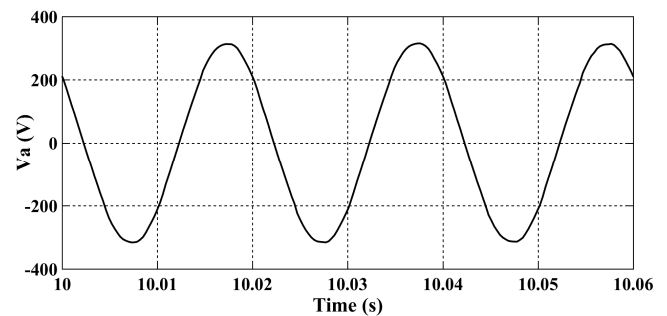Figure 20. Experimental waveform of D-STATCOM output current

Figure 21. Experimental waveform of PCC voltage

As shown in Fig. 22, at the 5th second asynchronous motor load of 1,5 kVAr, and 8th second asynchronous motor load of 1 kVAr has been activated in experimental study. In this case (at 8th) the modulation index increased from 0,9 to 1,05.
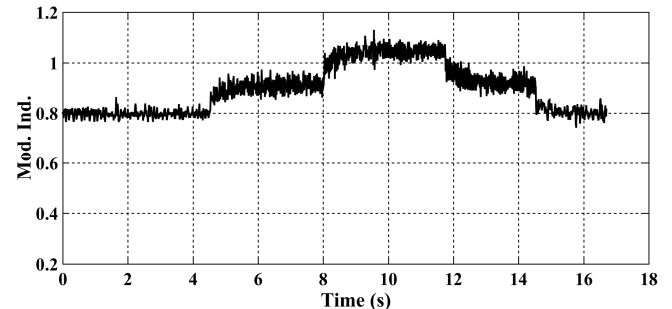
Figure 22. Experimental waveform of modulation index

3) Experimental Study 3

The same data in Experimental Study 2 is used for this study. Only the loads are connected to the system externally (without using the dSPACE ControlDesk environment). Fig. 23 shows the PCC voltage and current variations without D-STATCOM. Fig. 24 shows the PCC voltage and current variations with D-STATCOM. It is seen that there is no phase difference between current and voltage for analyzing the power factor.
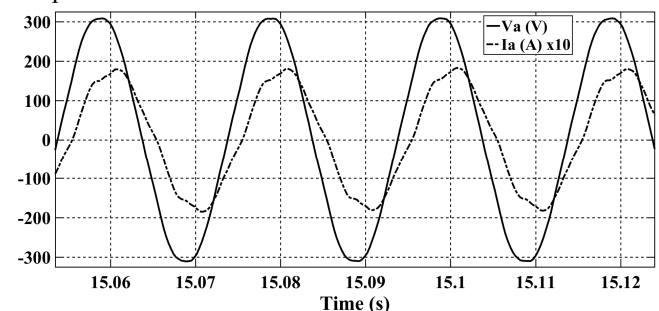
Figure 23. Experimental waveform of voltage and current at the PCC without D-STATCOM
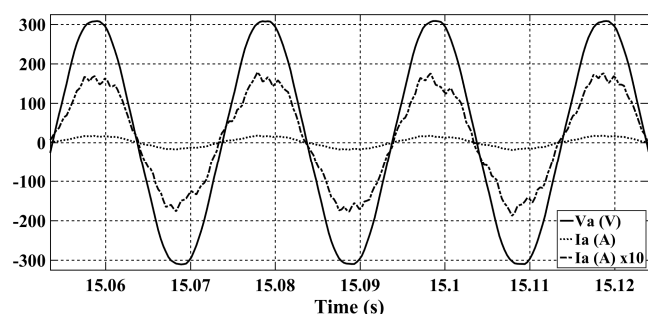
Figure 24. Experimental waveform of voltage and current at the PCC with D-STATCOM

Fig. 25 shows active and reactive powers at the PCC with D-STATCOM. As shown in Fig. 25, at 1.8th second 2kW resistive load, 5.25th second 2kW resistive load, 10.05th second asynchronous motor load of 5 kW and 14.7th second 2 kW resistive load has been activated. It is seen that the reactive power is 0 VAr as expected.
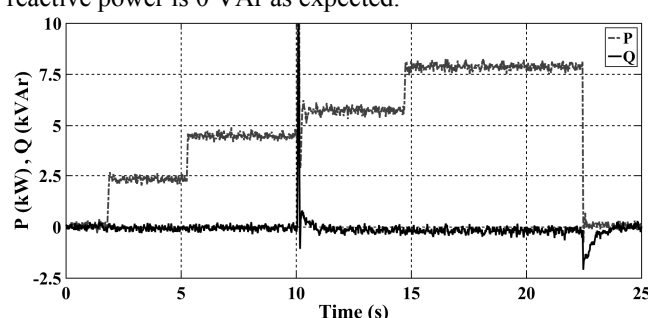

Figure 25. Experimental waveform of active and reactive powers

VII. Conclusion

This study has been carried out based on the cascaded H-bridge five level inverter-based D-STATCOM structure for wind energy systems. A new control circuit for controlling D-STATCOM device has been proposed. The dSPACE DS1104 platform has been used to implement the proposed control system. This platform allows working under the Matlab/Simulink environment. The proposed control scheme has been developed for D-STATCOM device to be used in wind power distribution systems. FLCM-PI controller is used to control the DC side of D-STATCOM and the *d* and *q* components of output current of D-STATCOM. Furthermore, by using the POD-SPWM technique, the output voltage is enhanced and the harmonic content of the voltage source inverter and voltage stress on inverter's switching elements are reduced.

The performance of D-STATCOM with the proposed control system is experimentally demonstrated for reactive power demand changes by connecting actual loads to the system (without using the dSPACE ControlDesk environment). From both simulation and experimental results, accurate reactive power compensation, voltage stability and quick response time are obtained by using the proposed control system. As can be seen from the graphs obtained, both simulation and experimental results overlap.

References

[1] J. M. Carrasco, L. G. Franquelo, J. T. Bialasiewicz, E. Galvan, R. C. P. Guisado, M. A. M. Prats, J. I. Leon, and N. M. Alfonso, "Power-Electronic Systems for the Grid Integration of Renewable Energy Sources: A Survey," IEEE Transactions on Industrial Electronics, vol. 53, no. 4, pp. 1002-1016, 2006. doi: 10.1109/TIE.2006.878356

[2] T. Ackermann, "Wind Power in Power Systems", pp. 257-282, John Wiley & Sons Ltd., 2005.

[3] P. Gonzalez, and A. Cerrada, "Control System for a PWM-based STATCOM," IEEE Trans. Power Delivery, vol. 15, pp. 1252-1257, 2000. doi: 10.1109/61.891511

[4] P. Rao, M. L. Crow, and Z. Yang, "STATCOM Control for Power System Voltage Control Applications," IEEE Transaction on Power Delivery, vol.15, no.4, pp. 1311-1317, 2000. doi: 10.1109/61.891520

[5] L. Lu, Z. Xie, X. Zhang, S. Yang, and R. Cao, "A Dynamic Wind Turbine Simulator of the wind turbine generator system," International Conference on Intelligent System Design and Engineering Appl., pp.967-970, 2012. doi: 10.1109/ISdea.2012.549

[6] J. Hussain, and M. K. Mishra, "Design and development of real-time small-scale wind turbine simulator," IEEE 6th India International Conference on Power Electronics, pp. 1-5, 2014. doi: 10.1109/IICPE.2014.7115782

[7] Md. Arifujjaman, M. T. Iqbal, and J. E. Quacioe, "Development of an Isolated Small Wind Turbine Emulator," The Open Renewable Energy Journal, pp. 3-12, 2011. doi: 10.2174/1876387101104010003

[8] A. Sokolovs, L. Grigans, E. Kamolins, and J. Voitkans, "An Induction Motor Based Wind Turbine Emulator," Latvian Journal of Physics and Technical Sciences, vol. 51, no. 2, pp. 11–21, May 2014. doi: https://doi.org/10.2478/lpts-2014-0009

[9] P. Rao, M. L. Crow, and Z. Yang, "STATCOM Control for Power System Voltage Control Applications," IEEE Transaction on Power Delivery, vol.15, no.4, pp. 1311-1317, 2000. doi: 10.1109/61.891520

[10] J.-S. Lai, and F. Z. Peng, "Multilevel converters-a new breed of power converters," IEEE Transactions on Industry Applications, vol. 32, no.3, pp. 509-517, 1996. doi: 10.1109/28.502161

[11] S. Kouro, M. Malinowski, K. Gopakumar, J. Pou, L. G. Franquelo, B.Wu, J. Rodriguez, M. A. Pérez, and J. I. Leon, "Recent advances and industrial applications of multilevel converters," IEEE Trans. Ind. Electron., vol. 57, no. 8, pp. 2553–2580, Aug. 2010. doi: 10.1109/TIE.2010.2049719

[12] A. Luo, C. Tang, Z. Shuai, J. Tang, X. Y. Xu, and D. Chen, "Fuzzy-PI based direct output-voltage control strategy for the STATCOM used in utility distribution systems," IEEE Trans. Ind. Electron., vol. 56, no. 7, pp. 2401–2411, Jul. 2009. doi: 10.1109/TIE.2009.2021172

[13] H. Akagi, S. Inoue, and T. Yoshii, "Control and performance of a transformerless cascade PWM STATCOM with star configuration," IEEE Trans. Ind. Appl., vol. 43, no. 4, pp. 1041–1049, Jul./Aug. 2007. doi: 10.1109/TIA.2007.900487

[14] Z. Xuehua, and S. Liping, "Current Decoupling Control Strategy of Medium Voltage Cascaded Multilevel STATCOM," Sensors and Transducers, vol.181, no. 10, pp. 101-110, October 2014.

[15] I. H. Altas, E. Ozkop, and A. M. Sharaf, "A novel active filter strategy for power mitigation and quality enhancements in a stand-alone WECS," International Conference on Electrical and Electronics Engineering, pp. I-88-I-91, 2009. doi: 10.1109/ELECO.2009.5355291

[16] F. Botteron, H. Pinheiro, H. A. Grundling, J. R. Pinheiro, and H. L. Hey, "Digital voltage and current controllers for three-phase PWM inverter for UPS applications," in Proc. IEEE Ind. Appl. Conf., pp. 2667–2674, Sep. 2001. doi: 10.1109/IAS.2001.955995

[17] W. Yao, H. Hu, and Z. Lu, "Comparisons of space-vector modulation and carrier-based modulation of multilevel inverter," IEEE Trans. Power Electron., vol. 23, no. 1, pp. 45–51, Jan. 2008.

[18] S. Wei, B. Wu, F. Li, and C. Liu, "A general space vector PWM control algorithm for multilevel inverters," in IEEE Appl. Power Electron. Conf. Expo., vol. 1, pp. 562–568, Feb. 2003. doi: 10.1109/APEC.2003.1179268

[19] V. G. Agelidis, A. Balouktsis, and M. S. A. Dahidah, "A five-level symmetrically defined selective harmonic elimination PWM strategy: Analysis and experimental validation," IEEE Trans. Power Electron., vol. 23, no. 1, pp. 19–26, Jan. 2008. doi: 10.1109/TPEL.2007.911770

[20] M. S. A. Dahidah, G. Konstantinou, and V. G. Agelidis, "SHE-PWM and optimized DC voltage levels for cascaded multilevel inverters control," in Proc. IEEE Symp. Ind. Electron. Appl., pp. 143–148, 2010. doi: 10.1109/ISIEA.2010.5679479

[21] H. Akagi, H. Fujita, S. Yonetani, and Y. Kondo, "A 6.6-kV transformerless STATCOM based on a five-level diode-clamped PWM converter: System design and experimentation of a 200-V 10-kVA laboratory model," IEEE Trans. Ind. Appl., vol. 44, no. 2, pp. 672–680, Mar./Apr. 2008. doi: 10.1109/IAS.2005.1518362

[22] Q. Song, W. Liu, and Z. Yuan, "Multilevel optimal modulation and dynamic control strategies for STATCOMs using cascaded multilevel inverter," IEEE Trans. Power Del., vol. 22, no. 3, pp. 1937–1946, Jul. 2007. doi: 10.1109/TPWRD.2007.899771

[23] K. Sano, and M. Takasaki, "A transformerless D-STATCOM based on a multivoltage cascade converter requiring no dc sources," IEEE

Trans. Power Electron., vol. 27, no. 6, pp. 2783–2795, Jun. 2012. doi: 10.1109/TPEL.2011.2174383

[24] H. Akagi, S. Inoue, and T. Yoshii, "Control and performance of a transformerless cascade PWM STATCOM with star configuration," IEEE Trans. Ind. Appl., vol. 43, no. 4, pp. 1041–1049, Jul./Aug. 2007. doi: 10.1109/TIA.2007.900487

[25] I. H. Altas, and A. M. Sharaf, "A generalized direct approach for designing fuzzy logic controllers in matlab/simulink gui envirement," international journal of information technology and intelligent computing, Int. J. IT&IC, no.4 vol.1, 2007.

[26] I. H. Altas, and O. O. Mengi, "A Fuzzy Logic voltage Controller for off-grid wind turbine supercapacitor renewable energy source," International Conference on Electrical and Electronics Engineering (ELECO), pp. 62-66, 2013. doi: 10.1109/ELECO.2013.6713804

[27] K. Yanmaz, I. H. Altas, and A. M. Sharaf, "Application of fuzzy reasoning based power filter and dynamic voltage regulator for single phase micro wind power generation systems," International symposium on innovations in intelligent systems and applications (INISTA), 2012. doi: 10.1109/INISTA.2012.6247004

[28] J. Xie, X. Kong, X. Huang, and Q. Yang, "Application of self-adaptive fuzzy PI control in the air-conditioning system," 2010 Chinese control and decision conference (CCDC), pp. 2999-3002, 2010. doi: 10.1109/CCDC.2010.5498653

[29] G. Wang, Z. Ping, J. Zhang, and Y. Guo, "Decoupling Control Strategy of D-STATCOM," Telkomnika, vol. 11, no. 6, pp. 3285-3292, 2013. doi: http://dx.doi.org/10.11591/telkomnika.v11i6.2684

[30] E. Sahin, I. H. Altas, "FPA Tuned Fuzzy Logic Controlled Synchronous Buck Converter for a Wave/SC Energy System" Advances in Electrical and Computer Engineering, vol. 17, no. 1, pp. 39-48, 2017. doi: 10.4316/AECE.2017.01006

[31] P. K. Jin, M. S. A. Dahidah, and C. Klumpner, "Nine-level SHE_PWM VSC based STATCOM for VAR compensation," in Proc. IEEE Int. Conf. Power Energy, 2010, pp. 135–140. doi: 10.1109/PECON.2010.5697570

[32] Q. Song, W. Liu, and Z. Yuan, "Multilevel optimal modulation and dynamic control strategies for STATCOMs using cascaded multilevel inverter," IEEE Trans. Power Del., vol. 22, no. 3, pp. 1937–1946, Jul. 2007. doi: 10.1109/TPWRD.2007.899771

[33] D. Masand, S. Jain, and G. Agnihotri, "Control strategies for distribution static compensator for power quality improvement," IETE Journal of Research, vol. 54, no. 6, pp. 421-428, Nov-Dec. 2008. doi: 10.4103/0377-2063.48632

[34] P. Sotoodeh and R. D. Miller, "Design and implementation of an 11-level inverter with FACTS capability for distributed energy systems," IEEE J. Emerg. Sel. Topics Power Electron., vol. 2, no. 1, pp. 87–96, Mar. 2014. doi: 10.1109/JESTPE.2013.2293311

[35] Z.Wang, B.Wu, D. Xu, and N. R. Zargari, "Hybrid PWM for high-power current-source-inverter-fed drives with low switching frequency," IEEE Trans. Power Electron., vol. 26, no. 6, pp. 1754–1764, Jun. 2011. doi: 10.1109/TPEL.2010.2087362

[36] P. Palanivel, S. S. Dash, "Analysis of THD and output voltage performance for cascaded multilevel inverter using carrier pulse width modulation techniques," IET Power Electronics, vol. 4, no. 8, pp. 951-958, 2011. doi: 10.1049/iet-pel.2010.0332

[37] P. Hamedani, A. Shoulaie, "A Comparative Study of Harmonic Distortion in Multicarrier Based PWM Switching Techniques for Cascaded H-Bridge Inverters," Advances in Electrical and Computer Engineering, vol. 16, no. 3, pp. 15-24, 2016. doi: 10.4316/AECE.2016.03003